



HAL
open science

Long-term elevated precipitation induces grassland soil carbon loss via microbe-plant–soil interplay

Mengmeng Wang, Xin Sun, Baichuan Cao, Nona Chiariello, Kathryn Docherty, Christopher Field, Qun Gao, Jessica Gutknecht, Xue Guo, Genhe He, et al.

► **To cite this version:**

Mengmeng Wang, Xin Sun, Baichuan Cao, Nona Chiariello, Kathryn Docherty, et al.. Long-term elevated precipitation induces grassland soil carbon loss via microbe-plant–soil interplay. *Global Change Biology*, 2023, 29 (18), pp.5429-5444. 10.1111/gcb.16811 . hal-04276539

HAL Id: hal-04276539

<https://agroparistech.hal.science/hal-04276539>

Submitted on 9 Nov 2023

HAL is a multi-disciplinary open access archive for the deposit and dissemination of scientific research documents, whether they are published or not. The documents may come from teaching and research institutions in France or abroad, or from public or private research centers.

L'archive ouverte pluridisciplinaire **HAL**, est destinée au dépôt et à la diffusion de documents scientifiques de niveau recherche, publiés ou non, émanant des établissements d'enseignement et de recherche français ou étrangers, des laboratoires publics ou privés.

1 **Long-term elevated precipitation induces grassland soil carbon loss via**

2 **microbe-plant-soil interplay**

3

4 Mengmeng Wang^{1,2†}, Xin Sun^{2,3,4,5†}, Baichuan Cao¹, Nona R. Chiariello⁶, Kathryn M.

5 Docherty⁷, Christopher B. Field⁸, Qun Gao², Jessica L. M. Gutknecht⁹, Xue Guo^{2,10},

6 Genhe He¹¹, Bruce A. Hungate¹², Jiesi Lei², Audrey Niboyet^{13,14}, Xavier Le Roux¹⁵,


7 Zhou Shi¹⁰, Wensheng Shu¹, Mengting Yuan¹⁰, Jizhong Zhou^{10,16,17,18*} and Yunfeng

8 Yang^{2*}


9

10 Mengmeng Wang  <https://orcid.org/0000-0002-1566-5895>


11 Xin Sun  <https://orcid.org/0000-0003-0280-4283>

12 Baichuan Cao  <https://orcid.org/0009-0003-8842-9193>


13 Christopher B. Field  <https://orcid.org/0000-0002-1684-8247>

14 Qun Gao  <https://orcid.org/0000-0002-2148-5807>

15 Jessica L. M. Gutknecht  <https://orcid.org/0000-0001-7667-5272>

16 Xue Guo  <https://orcid.org/0000-0002-4309-6140>

17 Bruce A. Hungate  <https://orcid.org/0000-0002-7337-1887>

18 Jiesi Lei  <https://orcid.org/0009-0000-0102-9540>

19 Audrey Niboyet  <https://orcid.org/0000-0003-3355-706X>

20 Xavier Le Roux  <https://orcid.org/0000-0001-9695-0825>

21 Zhou Shi  <https://orcid.org/0000-0002-9149-1540>

22 Wensheng Shu  <https://orcid.org/0000-0002-8743-1705>

23 Mengting Yuan  <https://orcid.org/0000-0003-0017-3908>

24 Jizhong Zhou  <https://orcid.org/0000-0003-2014-0564>

25 Yunfeng Yang  <https://orcid.org/0000-0001-8274-6196>

26

27 ¹Institute of Ecological Science and Guangdong Provincial Key Laboratory of
28 Biotechnology for Plant Development, School of Life Sciences, South China Normal
29 University, Guangzhou 510631, China.

30 ²State Key Joint Laboratory of Environment Simulation and Pollution Control, School
31 of Environment, Tsinghua University, Beijing 100084, China.

32 ³Department of Ecology and Evolutionary Biology, Yale University, New Haven, CT
33 06511, USA.

34 ⁴Yale Institute for Biospheric Studies, Yale University, New Haven, CT 06511, USA.

35 ⁵Department of Global Ecology, Carnegie Institution for Science, Stanford, CA 94305
36 USA.

37 ⁶Jasper Ridge Biological Preserve, Stanford University, Stanford, CA 94305, USA.

38 ⁷Department of Biological Sciences, Western Michigan University, Kalamazoo, MI
39 49008, USA.

40 ⁸Stanford Woods Institute for the Environment, Stanford University, Stanford, CA
41 94305, USA.

42 ⁹Department of Soil, Water, and Climate, University of Minnesota, Twin Cities, Saint
43 Paul, MN 55104, USA.

44 ¹⁰Institute for Environmental Genomics and Department of Microbiology and Plant

45 Biology, University of Oklahoma, Norman, OK 73019, USA.

46 ¹¹School of Life Sciences, Key Laboratory of Agricultural Environmental Pollution
47 Prevention and Control in Red Soil Hilly Region of Jiangxi Province, Jinggangshan
48 University, Ji'an 343009, China

49 ¹²Center for Ecosystem Science and Society, and Department of Biological Sciences,
50 Northern Arizona University, Flagstaff, AZ 86011, USA.

51 ¹³Sorbonne Université, Université Paris Cité, UPEC, CNRS, INRAE, IRD, Institut
52 d'Ecologie et des Sciences de l'Environnement de Paris, 75005, Paris, France

53 ¹⁴AgroParisTech, 91120, Palaiseau, France

54 ¹⁵Laboratoire d'Ecologie Microbienne, INRAE, CNRS, Université de Lyon, Université
55 Lyon 1, VetAgroSup, UMR INRAE 1418, UMR CNRS 5557, Villeurbanne, France

56 ¹⁶Earth and Environmental Sciences Division, Lawrence Berkeley National Laboratory,
57 Berkeley, CA 94720, USA.

58 ¹⁷School of Civil Engineering and Environmental Sciences, University of Oklahoma,
59 Norman, OK 73019, USA

60 ¹⁸School of Computer Science, University of Oklahoma, Norman, OK 73019, USA

61

62 †These authors contributed equally: Mengmeng Wang, Xin Sun

63 *To whom correspondence may be addressed. E-mail: jzhou@ou.edu; Phone:

64 1-405-325-6073; Fax: 1-405-325-7552; or yangyf@tsinghua.edu.cn; Phone:

65 +86-010-62784692; Fax: +86-010-62794006

66

67 **Running title:** Microbial responses to elevated precipitation

68 **Keywords:** elevated precipitation, soil carbon loss, microbial functional trait, viral

69 shunt, resource acquisition, water-limited ecosystems

70 **Type of article:** Research article

71

72 **Abstract**

73 Global climate models predict that the frequency and intensity of precipitation
74 events will increase in many regions across the world. However, the
75 biosphere-climate feedback to elevated precipitation (eP) remains elusive. Here, we
76 report a study on one of the longest field experiments assessing the effects of eP,
77 alone or in combination with other climate change drivers such as elevated CO₂
78 (eCO₂), warming, and nitrogen deposition. Soil total carbon (C) decreased after a
79 decade of eP treatment, while plant root production decreased after two years. To
80 explain this asynchrony, we found that the relative abundances of fungal genes
81 associated with chitin and protein degradation increased and were positively
82 correlated with bacteriophage genes, suggesting a potential viral shunt in C
83 degradation. In addition, eP increased the relative abundances of microbial stress
84 tolerance genes, which are essential for coping with environmental stressors.
85 Microbial responses to eP were phylogenetically conserved. The effects of eP on soil
86 total C, root production, and microbes were interactively affected by eCO₂.
87 Collectively, we demonstrate that long-term eP induces soil C loss, owing to changes
88 in microbial community composition, functional traits, root production, and soil
89 moisture. Our study unveils an important, previously unknown biosphere-climate
90 feedback in Mediterranean-type water-limited ecosystems, namely how eP induces
91 soil C loss via microbe-plant-soil interplay.

92

93 **Introduction**

94 The Anthropocene era has brought significant changes in Earth's precipitation
95 patterns (Shaw *et al.*, 2002). The global hydrologic cycle has intensified along with
96 climate warming (Huntington, 2006), leading to an increase in annual precipitation in
97 many regions during 1980–2019 (Gulev *et al.*, 2021). Extreme precipitation events
98 are anticipated to become more frequent in the 21st century (Corringham *et al.*, 2019,
99 Stevenson *et al.*, 2022). As water availability serves as a limiting factor for most
100 terrestrial ecosystems, the precipitation regime is a critical regulator of ecosystem
101 functioning in soils, which comprise the Earth's largest terrestrial C reservoir
102 (Reichstein *et al.*, 2013). However, how precipitation regime shifts will affect soil C
103 storage remains highly uncertain. To date, biogeochemical models have failed to
104 reproduce precipitation-related patterns of soil C dynamics (Falloon *et al.*, 2011),
105 hampering our ability to predict how future scenarios of altered precipitation will
106 influence soil C source or sink capacity.

107 The central west coast of North America, mainly in California, has a
108 Mediterranean-type climate regime characterized by hot, dry summers, and cool,
109 wet winters. The Jasper Ridge Global Change Experiment (JRGCE), which was
110 conducted in a California annual grassland, demonstrated that net primary
111 productivity (NPP) responded unimodally to variations in precipitation (Zhu *et al.*,
112 2016). A short-term (3-year) elevated precipitation (eP) treatment increased NPP,
113 primarily due to an increase in shoot production (Shaw *et al.*, 2002). However, the
114 positive shoot responses were largely offset by negative root responses, resulting in

115 an insignificant increasing trend in total NPP over a 5-year eP treatment (Dukes *et al.*,
116 2005). In addition, a study conducted in another California grassland revealed that
117 long-term trajectories of plant species richness and abundances of invertebrate
118 herbivores and predators differed from short-term responses to the eP treatment
119 (Sullivan *et al.*, 2016), suggesting that long-term eP treatment could restructure
120 ecological relationships that ultimately affect soils and soil biota.

121 Soil microorganisms respond more rapidly to changes in soil water content than
122 plants due to their faster intrinsic growth rates (Prosser *et al.*, 2007). In a study of
123 California grassland, soil active bacterial community examined by
124 meta-transcriptomic analysis was rapidly affected by a wet-up event within 1–72
125 hours, showing a consistent pattern conserved at the sub-phylum level (Placella *et al.*,
126 2012). At the DNA level, wetting decreased the relative abundance of *Actinobacteria*
127 but increased that of *Acidobacteria* (Barnard *et al.*, 2013). However, these responses
128 to short-term wetting were transient, displaying marked resilience. In contrast, fungal
129 communities were largely unaffected, suggesting that fungi might be more resistant
130 to changes in water availability. Furthermore, viral abundance in soils can be strongly
131 influenced by water availability (Williamson *et al.*, 2017).

132 Although numerous field experiments have explored the effect of short- or
133 mid-term eP treatment on the taxonomic composition of microbial communities, the
134 results have been inconsistent: microbial community composition was affected by eP
135 (3 years) (Ochoa-Hueso *et al.*, 2020), or not (2–8 years) (Docherty *et al.*, 2011,
136 Gutknecht *et al.*, 2012, Qi *et al.*, 2021). In addition, the functional potentials of soil

137 microbial communities, which underlie ecological processes, can be altered by eP. For
138 instance, precipitation-mediated changes in microbial communities were strongly
139 associated with increased soil respiration (Chou *et al.*, 2008). Soil nitrifying and
140 denitrifying enzyme activities, as well as the abundances of ammonia-oxidizing
141 bacteria and nitrite-oxidizing bacteria, were also altered by the eP treatment in the
142 JRGCE over 2–8 years since the experiment began (Barnard *et al.*, 2006, Horz *et al.*,
143 2004, Le Roux *et al.*, 2016, Niboyet *et al.*, 2011b). Increased soil N₂O emissions were
144 reported under eP, which were associated with increased denitrification rates (Brown
145 *et al.*, 2012). Similarly, changes in the abundances and enzyme activities of soil
146 denitrifiers were detected for a semi-arid grassland in response to
147 precipitation-mediated changes (Shi *et al.*, 2021).

148 Most studies examining soil microbial responses have focused on short-term eP
149 treatments. It remains unclear whether microbial communities adapt to long-term
150 altered soil moisture regimes as they do to elevated temperature (Melillo *et al.*,
151 2017), or whether they continue to shift in the long-term trajectories to differ from
152 short-term responses, as macrofauna and macroflora do (Sullivan *et al.*, 2016). To
153 address it, we examined plant and microbial responses (e.g., bacteria, fungi, and
154 viruses) to a 14-year eP treatment (+50%) alone or combined with elevated CO₂
155 (eCO₂, +275 μmol·mol⁻¹), warming (+1.0°C in topsoils) and nitrogen (N) deposition
156 (+7g·m⁻²·y⁻¹) in the JRGCE, one of the longest manipulations of precipitation in a
157 natural ecosystem. We hypothesized that long-term eP may lead to shifts in soil
158 microbial community composition and functional traits, contradicting the short-term

159 responses where eP affected microbial gene expression and physiology with no or
160 transient changes in microbial community composition (Barnard *et al.*, 2013,
161 Gutknecht *et al.*, 2012). We also hypothesized that the microbial responses to eP
162 might be interactively affected by other climate change factors such as eCO₂,
163 warming, and N deposition, as previously reported for plant production (Zhu *et al.*,
164 2016).

165

166 **Materials and Methods**

167 **Experimental design and soil sampling.** The JRGCE is located in an annual grassland
168 within a 481-ha protected area along the eastern foothills of the Santa Cruz
169 Mountains in northern California (37°40' N, 122°22' W). The mean annual
170 precipitation at the study site over 45 years was 604 mm, with more than 80% of
171 precipitation occurring as rain between November and March. The average annual
172 air temperature over 45 years was 13.4°C. The soil is a fine-loamy, mixed, thermic
173 Typic Haploxeralf, with a pH of 6.5-7.0 and a water-holding capacity of 21% (Brown *et al.*,
174 2012).

175 The JRGCE was established in October 1998 to evaluate grassland ecosystem
176 responses to global change treatments. The experiment consisted of eight blocks as
177 replicates, each with four circular plots of 3.14 m² area. Each plot was equally divided
178 into four quadrants, resulting in a total of 128 quadrants. To simulate the projected
179 future precipitation regime in the California grassland, half of the quadrants received
180 an additional 50% precipitation with sprinklers after each natural rainfall event, and

181 two additional watering events in the spring at the end of the rainy season to
182 simulate an extension of the rainy season by three weeks, while ambient
183 precipitation (aP) quadrants received no water addition, serving as controls. During
184 the 14 years of treatments preceding our study, ambient precipitation averaged 610
185 mm per year, and precipitation in the eP treatment averaged 870 mm (i.e. +42.6%,
186 Fig. S1A). In addition to elevated precipitation, the experiment included elevated
187 carbon dioxide (ambient vs. +275 $\mu\text{mol}\cdot\text{mol}^{-1}$ CO₂), warming (ambient vs. elevated
188 temperature by $\sim 1.0^\circ\text{C}$ in topsoils), and N deposition (ambient vs. +7 g N $\text{m}^{-2}\cdot\text{y}^{-1}$ as
189 Ca(NO₃)₂), all conducted in a full factorial design (Shaw *et al.*, 2002). The treatments
190 were arranged in a randomized block split-plot design, with warming and CO₂
191 elevation at the plot level and N deposition and eP assigned randomly at the subplot
192 level (Dahlin *et al.*, 2013, Gutknecht *et al.*, 2012). In 2003, an accidental wildfire
193 burned two of the eight blocks. In 2011, a controlled burn was carried out in half of
194 the blocks, including the two blocks burned in 2003, to provide a fire treatment.
195 Since previous studies found that fire significantly affected microbial communities
196 and ecosystem functioning across four global change treatments (Niboyet *et al.*,
197 2011a, Strong *et al.*, 2017, Yang *et al.*, 2020), the burned blocks were excluded from
198 the present analysis.

199 A total of 64 soil samples were collected on April 26th and 27th, 2012, 14 years
200 after the initial treatments were implemented. Soil samples were obtained by
201 collecting one 7 cm deep \times 5 cm diameter core from each quadrant and thoroughly
202 homogenizing the soil. These soil samples were then sieved through a 2 mm mesh

203 and stored at -20°C for geochemical analyses or at -80°C for microbial analyses.

204

205 **Environmental variables.** We determined soil total C and total N by combustion
206 analysis on a Carlo Erba Model 1500 CNS Analyzer (Carlo Erba Strumentazione, Milan,
207 Italy). Soil C: N ratios were then calculated as mass ratios of total C to total N. We
208 also collected soil total C and N data in 1998 (Year 0) and from 2000 (Year 2) to 2012
209 (Year 14) on a yearly basis. To measure soil temperature, we buried thermo-couples
210 at a depth of 2 cm in each quadrant and recorded hourly data, which we then
211 averaged over April 1st–27th, 2012 (Niboyet *et al.*, 2011b). We determined soil
212 moisture by comparing the mass of a 10-g soil sub-sample before and after drying at
213 105°C for one week. We measured soil pH by suspending 5 g of soil in 10 mL of
214 distilled water. We determined soil ammonium ($\text{NH}_4\text{-N}$) and nitrate ($\text{NO}_3\text{-N}$)
215 concentrations by suspending 5 g of soil in 50 mL of 2 M KCl solution, followed by
216 measuring filtered extracts using an Automated Segmented Flow Analyzer (SEAL
217 Analytical, Mequon, WI, USA). We collected soil CO_2 efflux data as previously
218 described (Strong *et al.*, 2017), which were measured from April 27th–29th to June
219 20th–25th, 2012.

220 The ecosystem NPP and its components, i.e., aboveground NPP (ANPP) and
221 belowground NPP (BNPP) were measured as previously described (Zhu *et al.*, 2016).
222 Specifically, we collected aboveground plant materials from a 141 cm^2 area of each
223 quadrant twice at the peak of standing biomass, once in mid-April to early May and
224 again in early to late May. The biomass was analyzed using a maximum of two

225 harvests to reduce phenological variation bias under different treatments. We
226 measured the total aboveground biomass by clipping all aboveground biomass,
227 separating individual plant species into functional groups: annual grass, perennial
228 grass, annual forb, and perennial forb (Gao *et al.*, 2021). We determined litter
229 biomass by collecting all senesced plant material from the ground within the same
230 area. After the first aboveground harvest, we determined belowground biomass by
231 taking four soil cores (2.5 cm diameter) in the same area, with two cores for shallow
232 roots (0–15 cm) and two for deep roots (15–30 cm). Fine roots in a depth of 0–15 cm
233 were separated from tap roots. All plant materials were oven-dried at 70°C and
234 weighed. NPP, ANPP, and BNPP data in 1998 and from 2000 to 2011 (BNPP and NPP
235 in 1999 and 2007 not available) were also collected as previously described (Zhu *et*
236 *al.*, 2016).

237

238 **DNA extraction, purification, and quantification.** We extracted soil DNA by
239 freeze-grinding mechanical lysis, as previously described (Zhou *et al.*, 1996). We
240 purified DNA with a 0.5% low-melting-point agarose gel electrophoresis followed by
241 phenol-chloroform-butanol extraction. We assessed DNA quality using absorbance
242 ratios of 260/280 nm and 260/230 nm ($260/280 > 1.8$ and $260/230 > 1.7$) with a
243 NanoDrop ND-1000 Spectrophotometer (NanoDrop Technologies, Wilmington, DE,
244 USA). We then quantified the final DNA concentration with a PicoGreen method,
245 using an FLUO star Optima (BMG Labtech, Jena, Germany) as previously described
246 (Yang *et al.*, 2014).

247

248 **MiSeq sequencing and raw data preprocessing.** We constructed the 16S rRNA gene
249 library and processed sequencing data as previously described (Guo *et al.*, 2019). We
250 targeted the V4 region of the 16S rRNA gene with primers 515F
251 (GTGCCAGCMGCCGCGGTAA) and 806R (GGACTACHVGGGTWTCTAAT) and ITS2 region
252 between 5.8S and 28S rRNA genes with primers gITS7 (GTGARTCATCGARTCTTTG) and
253 ITS4 (TCCTCCGCTTATTGATATGC) in PCR amplification. We then sequenced PCR
254 products by 2 × 250 bp paired-end sequencing with a MiSeq instrument (Illumina,
255 San Diego, CA, USA). We identified paired-end raw sequences by paired barcodes and
256 combined them using FLASH (Magoč & Salzberg, 2011). We further trimmed
257 sequences to the length of > 245 bp for the 16S rRNA gene or >220 bp for the ITS. We
258 generated amplicon sequence variants (ASVs), also known as zero-radius operational
259 taxonomic units or unique sequence variants, by UNOISE3 (Edgar, 2018). We
260 annotated the representative sequence taxonomy using the QIIME2 Naive Bayes
261 classifier trained for the V4 region of the 16S rRNA gene (version
262 Silva-132-99-515-806) and ITS based on UNITE QIIME release (version
263 ver8_97_10.05.2021) (Abarenkov *et al.*, 2021, Quast *et al.*, 2013). We removed the
264 singlet ASVs and those classified as mitochondria and chloroplasts to improve data
265 reliability. We retrieved 3,391,680 high-quality sequences for the 16S rRNA gene and
266 661,632 high-quality sequences for ITS. Then, we resampled 16S rRNA gene
267 sequences at a depth of 31,441 reads and ITS sequences at a depth of 17,397 reads
268 for each of the 64 samples (Fig. S2). The representative 16S rRNA gene sequences

269 were aligned using MAFFT and used for constructing phylogenetic trees by FastTree
270 on QIIME2 (Bolyen *et al.*, 2019). Although the ITS2 region has a high resolution for
271 identifying evolutionarily close taxa, the high rate of insertion and deletion makes
272 the evolutionarily distant taxa vary greatly and difficult to be aligned. Therefore, we
273 constructed the fungal phylogenetic tree by specifying constraint alignment in
274 FastTree v2.1.10 (Price *et al.*, 2010). The constraint alignment was converted from a
275 guide tree constructed using ghost-tree (Fouquier *et al.*, 2016), which grafted the
276 taxonomically assigned ITS sequences to a reference foundation tree (Silva Ver. SSU
277 138) by mapping genus names.

278

279 **GeoChip experiments and raw data preprocessing.** We carried out DNA labeling
280 with Cy3 and hybridization with the functional array GeoChip 4.6, as previously
281 described (Wang *et al.*, 2018). We scanned the fluorescent intensities of each probe
282 on GeoChip, using a NimbleGen MS 200 Microarray Scanner with 100% laser power
283 and 100% photomultiplier tube (Roche, Basel, Switzerland). We discarded spots with
284 a signal-to-noise ratio of less than 2.0. Probe signals that were detected only once
285 among four biological replicates were also excluded. As a result, a total of 60,619
286 probes, including 53,748 probes derived from bacteria, 4,661 probes from
287 eukaryotes, 1,821 probes from archaea, and 389 from viruses, were detected. We
288 performed a natural logarithmic transformation of each detected probe (a_{ij}) (probe
289 $j \in [1, 60619]$, sample $i \in [1, 64]$) to get $b_{ij} = \ln(a_{ij} + 1)$ (we added 1 to a_{ij}
290 because the natural logarithm of zero is not defined). We normalized b_{ij} by dividing

291 the average signal intensity of all probes in the sample i to get $c_{ij} = b_{ij}/\text{Avg}_{j=1}^m b_{ij}$
292 (m is the total number of probes, i.e. 60,619).

293

294 **Statistical analyses.** All statistical analyses were performed in R version 3.5.2
295 (<http://www.r-project.org>) unless otherwise specified. P -values < 0.050 are
296 considered to be statistically significant. P -values between 0.050 and 0.100 are
297 considered to be marginally significant, given the large variations among blocks.
298 P -values > 0.100 are not considered to be statistically significant.

299

300 *Diversity analyses.* We calculated the α -diversity of the Shannon index for taxonomic
301 diversity (based on rarefied ASV tables) and functional gene diversity (based on
302 functional genes of GeoChip), and Faith's phylogenetic diversity. We utilized the
303 *vegan* and *picante* packages for these analyses.

304

305 *Treatment effect analyses.* To assess the treatment effect, we calculated the effect
306 size of precipitation as follows: % effect = $100\% \times (eP - aP)/aP$ ($n = 64$ under eP and
307 aP for data in 1998 and 2000–2003 before the 2003 fire, $n = 48$ for data in
308 2004–2011 before the 2011 fire, and $n = 32$ for data in 2012). The statistical
309 significance of the treatment effect was tested by split-plot ANOVA using *aov*
310 function in R. We applied log or square root transformations to improve normality
311 when necessary. To analyze the treatment effect on functional and taxonomic
312 compositions of microbial communities, we performed split-plot PERMANOVA with

313 PRIMER 6 + PERMANOVA software (Marti *et al.*, 2008). We used negative binomial
314 models in the DESeq2 package to identify significantly changed ASVs with eP
315 (baseMean > 10, log₂ fold change > 0.5, and FDR adjusted *P* value < 0.050), and
316 examined the significance with Wald tests (Love *et al.*, 2014). Using DESeq2 and
317 split-plot ANOVA, we also examined the effects of the eP treatment across different
318 taxonomic levels to determine whether the alterations in taxonomic lineages were
319 phylogenetically clustered. We adjusted *P*-values using the FDR method when
320 conducting multiple comparisons, such as assessing the eP effect on multiple
321 functional genes and taxonomic lineages.

322

323 *ConsenTRAIT analysis.* We performed consenTRAIT analysis to determine whether
324 the responses of bacteria and fungi to eP were phylogenetically conserved, using the
325 castor package (Louca & Doebeli, 2018, Martiny *et al.*, 2013). Since FastTree only
326 estimates branch lengths by inferring approximately-maximum-likelihood
327 phylogenetic trees, we constructed a maximum likelihood (ML) tree of the 16S rRNA
328 gene sequences to obtain accurate branch lengths for the consenTRAIT analysis. For
329 ITS sequences, it is difficult to align the sequences and construct an ML tree because
330 of high variations, we constructed the phylogenetic tree using constrained FastTree's
331 topology search instead.

332

333 *Ecological process analyses.* Microbial community assemblies are shaped by
334 ecological processes, including both stochastic processes (e.g., dispersal, birth-death

335 events, and ecology drift) and deterministic processes (e.g., environmental filtering)
336 (Hubbell, 2001, Ning *et al.*, 2019). We estimated the stochastic ratio using a modified
337 method based on null-model algorithms with taxonomic metrics (Sorensen) as
338 previously described (Guo *et al.*, 2018, Ning *et al.*, 2019). The effect of the eP
339 treatment on the estimated stochastic ratio was evaluated by split-plot
340 permutational multivariate analysis of variance (PERMANOVA).

341

342 *Structural equation modeling and aggregated boosted tree analyses.* Structural
343 equation modeling (SEM) was employed to reveal how biotic and abiotic variables
344 affect soil total C across aP and eP quadrants. Since soil total C was altered by both
345 eP and N deposition (Table S1), only samples under the ambient N condition (a total
346 of 32 samples) were used for SEM analysis to exclude the effect of N deposition. The
347 community compositions were represented by PC1 from the principal coordinate
348 analysis based on the Bray-Curtis dissimilarity of the ASV matrix, which captured 9.3%
349 - 15.5% variations of microbial community composition. We first established a full
350 model with all reasonable pathways (Fig. S3), and then we used a stepwise approach
351 to remove non-significant pathways with the highest *P*-value at each step until the
352 final model was obtained. The SEM analysis was performed using the lavaan R
353 package (Rosseel, 2012).

354 We performed the aggregated boosted tree (ABT) analysis, a machine learning
355 algorithm, to investigate the relative influences of biotic and abiotic variables in
356 regulating soil total C (De'ath, 2007). We first established a hyper grid of parameters,

357 including learning rate (shrinkage), interaction depth, the minimum number of
358 observations in the terminal nodes of trees (n.minobsinnode), and subsampling
359 fraction (bag.fraction), for tree training and tuning (Data S1). However, when
360 shrinkage was set to 0.001, the optimal trees became too large, which might lead to
361 overfitting of the ABT models. Therefore, we opted for the optimal combination of
362 parameters, which included shrinkage = 0.01, interaction depth = 1, n.minobsinnode
363 = 3, and bag.fraction = 0.8. Finally, we evaluated the model by 10-fold
364 cross-validation. ABT models were built by gbm function in gbm R package, and
365 model evaluation was performed by train function in caret R package.

366

367 **Results**

368 **Edaphic and plant variables**

369 The eP treatment did not change soil total C in the early phase of the 2nd–9th year
370 since the experiment began (Fig. 1A & Table S2). In the late phase of the 10th–14th
371 year, eP decreased soil total C by 4.2% ($P < 0.001$, Fig. 1A & Table S2), with significant
372 eP effects on soil total C in the 10th, 13th, and 14th year ($P < 0.021$, Fig. S1B). Soil total
373 N was not altered by eP alone (Fig. 1B & Table S2). As a result, the C: N ratio was
374 significantly decreased by eP ($P = 0.002$, Fig. 1C & Table S2). Treatment effects on
375 other soil variables were described in Supplementary Text A.

376 Aboveground net primary production (ANPP) was increased from 591 g·m⁻²·y⁻¹ in
377 ambient precipitation (aP) quadrants to 632 g·m⁻²·y⁻¹ in eP quadrants throughout the
378 2nd–14th year ($P = 0.018$, Fig. 1D & Table S2). In contrast, belowground NPP (BNPP)

379 was decreased from $463 \text{ g}\cdot\text{m}^{-2}\cdot\text{y}^{-1}$ in aP quadrants to $401 \text{ g}\cdot\text{m}^{-2}\cdot\text{y}^{-1}$ in eP quadrants (P
380 < 0.001 , Fig. 1D & Table S2). The decline in BNPP counterbalanced the increase in
381 ANPP, resulting in an unchanged NPP by the eP treatment (Fig. 1D). However, eP
382 effects on ANPP and BNPP varied considerably by year (Fig. S1C & S1D). ANPP was
383 significantly increased in only two years of the 14-year observations (Fig. S1C), while
384 BNPP was significantly decreased by 14.9%–25.2% during the first 2nd–5th years ($P <$
385 0.021 , Fig. S1D). However, the decline in BNPP was only observed in three years
386 during the late 6th–14th years (Fig. S1D).

387 There was an interactive effect of precipitation \times warming on soil total C ($P =$
388 0.048 , Table S2), which was decreased by eP when the temperature was ambient but
389 was unaltered by eP when the temperature was elevated (Fig. 1E). In the early phase
390 of the 2nd–9th year, soil total C was not altered by eP alone or combined with other
391 global change factors (Table S2). In contrast, soil total C was interactively affected by
392 precipitation \times CO₂ \times warming in the late phase of the 10th–14th year ($P = 0.008$, Table
393 S2), leading to a decline in soil total C under eP when CO₂ or temperature was
394 elevated (Fig. 1F). Soil CO₂ efflux was measured in the 14th year of the experiment.
395 Soil CO₂ efflux was interactively affected by precipitation \times CO₂ \times N deposition ($P =$
396 0.022 , Table S3), with eP increasing CO₂ efflux when CO₂ was elevated and N was
397 ambient (Fig. 1G). Soil total N was interactively affected by precipitation \times N
398 deposition \times warming ($P = 0.047$, Table S2), with eP decreasing soil total N only under
399 N deposition and ambient temperature (Fig. 1B). BNPP and NPP were interactively
400 affected by precipitation \times CO₂ \times warming ($P < 0.037$, Table S2), with eP decreasing

401 BNPP when CO₂ and temperature were elevated (Fig. 1H) and decreasing NPP when
402 CO₂ was elevated and the temperature was ambient (Fig. 1I).

403

404 **Microbial functional genes**

405 To examine the shifts in microbial communities by long-term eP, we analyzed
406 microbial functional potentials with functional gene array (GeoChip 4.6) and
407 prokaryotic and fungal community compositions with targeted amplicon sequencing,
408 using soil samples collected in the 14th year of the experiment. Microbial functional
409 gene composition differed between the aP and eP quadrants ($P = 0.050$, Table S4),
410 though functional gene α -diversity remained similar (Table S5). There were
411 interactive effects of precipitation \times CO₂ on functional gene composition and
412 α -diversity (Table S4 & S5). Functional gene α -diversity increased with eP when CO₂
413 was elevated, while it was not affected by eP when CO₂ was ambient (Fig. S4).

414 The relative abundances of genes associated with the degradation of pectin
415 (*pme*) and cellulose (the gene encoding endoglucanase derived from bacteria) were
416 decreased in the eP quadrants ($P < 0.025$, Fig. 2A). In contrast, the relative
417 abundances of fungal genes encoding enzymes related to the degradation of N-rich
418 compounds, such as chitin (endochitinase) and protein (aspartate protease and
419 serine protease), were increased by 4.4%–18.1% with eP ($P < 0.025$, Fig. 2A). In
420 addition, the relative abundance of the marker gene for methanogenesis (*mcrA*)
421 increased ($P = 0.017$) under eP, while those of methane oxidation genes *mmoX* and
422 *pmoA* were unaltered (Fig. S5A). There were interactive effects of precipitation \times CO₂

423 on C degradation genes, but not methane cycling genes (Data S2). Notably, the
424 increase in relative abundances of genes associated with degrading N-rich
425 compounds was greater when CO₂ was elevated (Fig. S6A). Taken together, these
426 results suggest that eP substantially altered soil microbial C cycling potentials,
427 especially when CO₂ was elevated.

428 Since bacteriophages play an important role in regulating microbial C dynamics,
429 we investigated 221 bacteriophage genes detected in our samples. The relative
430 abundances of bacteriophage genes associated with viral structure and replication
431 increased by 4.7%–9.5% in eP quadrants ($P < 0.040$, Fig. 2B), suggesting that eP may
432 stimulate bacteriophage growth. . In contrast, the total abundances of 101
433 eukaryotic viral genes detected in our samples remained unaltered (Fig. 2B). There
434 were interactive effects of precipitation × CO₂ on bacteriophage genes (Data S2),
435 whose gene abundances increased with eP when CO₂ was elevated (Fig. S6B).

436 Since long-term eP decreased soil total C, we investigated whether microbial
437 stress responses were stimulated. The relative abundances of eight stress response
438 genes were significantly increased with eP (Fig. 2C), including those associated with
439 glucose limitation, oxygen limitation, phosphate limitation, oxidative stress, and
440 sigma factors (see Supplementary Text B for details). There were interactive effects of
441 precipitation × CO₂ on phosphate limitation and sigma factor genes (Data S2), whose
442 gene abundances increased with eP when CO₂ was elevated and the temperature
443 was ambient (Fig. S6C & S4D).

444

445 **Microbial taxonomic composition**

446 We identified 4,649 to 14,940 prokaryotic amplicon sequence variants (ASVs) and
447 719 to 1,757 fungal ASVs per sample (Fig. S2). Their taxonomic compositions were
448 different between the eP and aP quadrants ($P = 0.001$), but were barely affected by
449 the interaction of precipitation and other climate change treatments (Table S4). The
450 taxonomic and phylogenetic α -diversities remained unaltered between the eP and aP
451 quadrants (Table S5).

452 Positive eP responders of bacteria, i.e., bacterial ASVs increased by eP, were
453 clustered within *Bacteroidetes*, *Gammaproteobacteria*, the order *Sphingomonadales*
454 of *Alphaproteobacteria*, and the order *Blastocatellales* of *Acidobacteria* (Fig. 3 & Data
455 S3, see Supplementary Text C for details). Negative eP responders of bacteria, i.e.,
456 bacterial ASVs decreased by eP, were clustered within *Actinobacteria*,
457 *Verrucomicrobia*, *Chloroflexi*, subgroup6 of *Acidobacteria*, and the family
458 *Beijerinckiaceae* of *Alphaproteobacteria* (Fig. 3 & Data S3). The positive and negative
459 eP responders were phylogenetically clustered in these clades at a greater depth
460 than expected in a null model of consenTRAIT analysis ($P < 0.001$, Table 1),
461 suggesting that the bacterial community's response to long-term eP was
462 phylogenetically conserved.

463 Positive eP responders of fungi were clustered within the class *Sordariomycetes*
464 and the order *Eurotiales* of *Ascomycota* (Fig. 4 & Data S4). Negative eP responders of
465 fungi were clustered in the class *Archaeorhizomycetes*, the order *Onygenales*,
466 *Helotiales*, and *Orbiliiales*, the family *Periconiaceae* and *Herpotrichiellaceae* of

467 *Ascomycota*, and the order *Agaricales* of *Basidiomycota* (Fig. 4 & Data S4). The
468 negative eP responders of fungi were phylogenetically conserved in deep-rooting
469 clades ($P = 0.003$), however, the positive eP responders were not, as indicated by the
470 absence of significant phylogenetic conservation (Table 1).

471

472 **Ecological processes in shaping microbial community assembly**

473 The phylogenetically conserved response of microbial communities to eP implies that
474 environmental filtering, a deterministic process, may be important under eP. To test
475 this, we estimated the relative importance of stochastic and deterministic processes
476 using a null model analysis. There were interactive effects of precipitation \times CO₂ on
477 the stochastic ratios of bacterial communities ($P = 0.004$), which decreased with eP
478 when CO₂ was elevated ($P = 0.031$) but remained unaltered with eP when CO₂ was
479 ambient (Fig. 5A). In contrast, stochastic ratios of fungal community decreased with
480 eP regardless of CO₂ conditions (Fig. 5B), showing higher environmental selection.

481 To identify the deterministic factors that affect microbial community
482 composition, we conducted Mantel tests to examine the linkages between
483 environmental variables and microbial eP responders. The positive eP responders of
484 fungi and negative eP responders of bacteria were both correlated with soil moisture
485 and soil CO₂ efflux (*Mantel's* $r = 0.149\text{--}0.203$, $P < 0.015$, Fig. 5C). In contrast, the
486 negative eP responders of fungi and positive eP responders of bacteria were
487 correlated with environmental variables to a lesser degree (see Supplementary Text
488 D for details). We also examined the linkages between environmental variables and

489 stress response genes and found that stress response genes were correlated with soil
490 total C, soil total N, and litter biomass (*Mantel's* $r = 0.101-0.267$, $P < 0.050$, Fig. 5C).

491

492 **Biotic and abiotic variables linking to soil total C**

493 Since soil total C decreased with long-term eP, we identified biotic and abiotic
494 variables that could be major drivers of soil total C. Structural equation modeling
495 (SEM) analyses were performed with the presumed relationships (Fig. S3) among the
496 selected subsets of edaphic and plant variables that were least correlated (see
497 Methods for details of model selection). Soil total C was negatively affected by soil
498 moisture but positively affected by fine root biomass (Fig. 6A). Soil total C was
499 significantly correlated with fungal community composition, which was, in turn,
500 correlated with relative abundances of genes associated with the degradation of
501 N-rich chitin and protein. The relative abundances of bacteriophage genes had a
502 strong correlation with those of C degradation genes, likely revealing an important
503 role of viral shunt on soil C cycling. Overall, these variables explain 54% of the
504 variations in soil total C (Fig. 6A). Among all the tested independent variables, soil
505 moisture, fine root biomass, and fungal community composition played essential
506 roles in mediating soil total C, as revealed by both SEM and aggregated boosted tree
507 (ABT) analysis (Fig. 6A & 6B). Soil pH and enriched microbial C degradation genes
508 influenced soil total C to lesser extents. These results indicate that soil, plant, and
509 microbial variables explain a similar proportion of soil total C dynamics.

510

511 **Discussion**

512 Understanding how long-term climate changes affect soil microbial communities and
513 underlying ecosystem processes is essential for better predicting the terrestrial
514 responses to climate change (Tiedje *et al.*, 2022). By examining the effects of
515 14-years eP on edaphic variables, plants, bacteria, fungi, and viruses, our study
516 provides explicit evidence that long-term eP, either alone or in combination with
517 other climate change drivers, can alter ecosystem compositions and functional traits
518 linked to soil C loss.

519

520 **The long-term eP treatment shifts microbial community compositions and**
521 **functional traits**

522 Although the short- or mid-term (3–8 years) eP treatment in the JRGCE did not alter
523 microbial community composition (Docherty *et al.*, 2011, Gutknecht *et al.*, 2012), we
524 found that bacterial and fungal community compositions were significantly changed
525 after 14-year eP treatment (Table S4). This result supports our hypothesis that
526 microbial communities continue to shift in the long-term trajectories, differing from
527 short-term responses (Sullivan *et al.*, 2016). However, this discrepancy could also be
528 attributed to technical differences. Previous studies, which relied on low-resolution
529 microbial community fingerprinting based on lipid biomarker analysis, may not unveil
530 variations in microbial community composition (Docherty *et al.*, 2011, Gutknecht *et*
531 *al.*, 2012). Our analysis offers supporting evidence that microbial responses to water
532 availability are phylogenetically clustered (Table 1) (Placella *et al.*, 2012, Xu *et al.*,

533 2018), which could reflect the fundamental differences in microbial life strategies, i.e.,
534 traits driving survival, growth, and reproduction responses to environmental
535 conditions (Barnard *et al.*, 2013).

536 The phylogenetic conservation of microbial communities could be attributed to
537 stress tolerance and competition-related traits (Goberna *et al.*, 2014). In support of
538 stronger stresses, the stochastic ratios of prokaryotic and fungal communities were
539 decreased by the eP treatment (Fig. 5A & 5B). In addition, stress tolerance genes
540 increased in relative abundances with long-term eP (Fig. 2C), reflecting higher
541 environmental stress. For example, increases in oxygen limitation gene abundances
542 might result from less oxygen in soil pore space or diffusing in the water film under
543 eP (Schuur & Matson, 2001), while oxidative stress levels could be increased when
544 microbes are under stress (Ernst *et al.*, 2022).

545 The functional traits related to C degradation were shifted towards the
546 degradation of N-rich compounds (such as chitin and protein), but not chemically
547 C-rich compounds (such as starch, pectin, and hemicellulose, Fig. 2A). These results
548 were consistent with previous results in the JRGCE showing that 6-year eP treatment
549 decreased hydrolase activity in degrading starch, xylan, and cellulose, but was
550 inconsistent with a previous result of decreased chitin hydrolase activity (Henry *et al.*,
551 2005). The discrepancies in chitin degradation might be due to variations in C
552 degradation trait over different time scales or technical differences since our results
553 reflect the genetic potentials for these processes, while enzyme activities reflect the
554 maximum potential under ideal conditions. Degradation of N-rich molecules,

555 including chitin and proteins, also increased along a precipitation gradient from arid
556 to semi-arid grasslands (Feng *et al.*, 2018), which could reflect a microbial need for
557 acquiring N nutrients.

558 Viral shunt, which releases organic matter from microbial cells, plays an
559 important role in regulating C and N cycling across different ecosystems such as
560 marine and anaerobic digesters (Coutinho *et al.*, 2017, Zhang *et al.*, 2017).
561 Consistently, the relative abundance of bacteriophage genes was increased with eP
562 (Fig. 2B & Fig. S5B), and were positively correlated with genes associated with the
563 degradation of chitin and protein and consequently affected soil total C (Fig. 6A).
564 Those results suggest that bacteriophages might play an important role in C cycling of
565 our annual grassland ecosystem. However, we cannot yet identify the host of the
566 bacteriophages, hindering closer examinations of interactions among bacteria and
567 bacteriophages.

568

569 **The long-term eP treatment effects are interactively affected by elevated CO₂ and**
570 **warming**

571 Elevated CO₂ enhanced eP effects on microbial functional traits and bacterial
572 community assemblies in this study (Fig. S6 & Fig.5A). One possible explanation is
573 that CO₂ fertilization could induce higher shortages for other resources such as N and
574 phosphorus, according to the ecological framework of (co)limitation by multiple
575 resources (Ma *et al.*, 2019). Also, both eCO₂ and eP could decrease root biomass
576 (Iwasa & Roughgarden, 1984, Shaw *et al.*, 2002), consequently reducing root input to

577 the soil and causing soil nutrient limitation (Mason *et al.*, 2022, Shaw *et al.*, 2002).
578 Consistently, we found that eP in combination with eCO₂ decreased BNPP and even
579 NPP (Fig. 1H & 1I). Nitrogen and phosphorus limitation was supported because we
580 revealed enhanced degradation of N-rich compounds (Fig. S6A) and decreased N
581 cycling under eP when CO₂ was elevated (Fig. S7), as well as increased phosphate
582 limitation genes (Fig. S6C). Alternatively, it is possible that eCO₂ decreases
583 evapotranspiration, prolongs the period of water conserved in the soil, and increased
584 soil moisture, as already observed in JRGCE and semi-arid shortgrass steppe of
585 Colorado (Nelson *et al.*, 2004, Zavaleta *et al.*, 2003), hence enhancing the eP effect
586 on microbial communities and ecosystem functioning.

587 Warming mitigated eP effects on soil total C and precipitation × CO₂ effects on
588 plant root production and phosphate limitation genes (Fig. 1E, 1I & S4C). This could
589 happen because increased evapotranspiration under warming could reduce water
590 availability and the duration of water conserved in soil. Meanwhile, warming could
591 enhance organic phosphorus and N mineralization to ameliorate nutrient limitation
592 (Liu *et al.*, 2017, Shaw & Cleveland, 2020), although the increase in N mineralization
593 rate in response to warming has not yet been observed at our study site (Gao *et al.*,
594 2021, Niboyet *et al.*, 2011b).

595

596 **Microbe-plant-soil interplay is essential for mediating eP-induced soil C loss**

597 The eP treatment reduced soil total C in the JRGCE from the 10th year of the
598 experiment, with only a reduction in the free light fraction of soil organic matter

599 –mainly root materials– being observed after the 6-year eP treatment (Henry *et al.*,
600 2005), indicating that long-term eP exacerbated soil C loss. Since soil inorganic C
601 content is stable in areas where mean annual precipitation is greater than 600 mm,
602 and an increase in water availability has little effect on soil inorganic C in acidic or
603 neutral soils (Dang *et al.*, 2022), the decrease in soil total C in this study might be
604 mainly attributed to the decrease in soil organic C. This result contradicts the
605 increase in soil organic C pools with higher precipitation on the North American
606 Great Plains (Derner & Schuman, 2007, Morrow *et al.*, 2017). A possible explanation
607 is that the eP effect on soil C is mediated by primary production. Increased
608 precipitation on the Great Plains led to soil C gain by supporting plant photosynthesis
609 (Flanagan *et al.*, 2002), but the NPP in the JRGCE was not altered by the eP treatment
610 due to decreases in root production, offsetting increases in shoot production (Fig. 1D)
611 (Dukes *et al.*, 2005). Root production may decline due to reduced allocation to roots
612 as soil resources become more available according to the optimal shoot-root C
613 allocation theory (Iwasa & Roughgarden, 1984). Alternatively, it might be due to the
614 suppressed root respiration as soils occasionally become waterlogged in the eP
615 treatment (Dukes *et al.*, 2005). Since root exudates and decomposing root residues
616 are large contributors to soil C pool, the decrease in root production likely explained
617 the observed decrease in soil total C in our study (Fig. 6). Notably, the decrease in
618 root production was consistent only during the first few years (2nd–5th years) of eP
619 treatment but not over longer terms (6th–14th years, Fig. S1D). The decoupled
620 decreases in root production and soil C (Fig. S1) may indicate a legacy effect of root

621 biomass on soil total C via C-aggregate and C-mineral associations (Sokol *et al.*,
622 2022).

623 Microbial traits, such as resource acquisition and stress tolerance, can mediate
624 soil C cycling (Malik *et al.*, 2020). In resource-limited and abiotic-stressed
625 environments, microbes tend to prioritize costly resource acquisition or stress
626 tolerance over high growth yield, resulting in polymer decomposition and soil C loss
627 observed in this study (Fig. 5C & 6) and elsewhere (Malik *et al.*, 2020, Malik *et al.*,
628 2018). In addition, the enhanced microbial decomposition of soil C under eP may be
629 responsible for soil C loss (Nielsen & Ball, 2015). Heterotrophic respiration could be
630 positively affected by eP, especially under eCO₂ and ambient N deposition (Fig. 1F).
631 Increased water availability can stimulate microbial activity, growth, and respiration,
632 leading to a lasting effect on soil C loss (Nielsen & Ball, 2015, Wang *et al.*, 2015).
633 Moreover, the eP treatment altered microbial community composition, consistent
634 with changes in microbial community preference for different C substrates (Zhou *et al.*,
635 2012). Higher abundances of fungal taxa (Fig. 4 & Data S4) and C-degrading genes
636 (Fig. 2A & Fig. S8) suggest that fungi become increasingly important for degrading C
637 under the long-term eP treatment, as supported by the SEM and ABT analyses (Fig.
638 6). Consistently, the abundances of *Eurotiales* and *Sordariales*, the positive eP
639 responders of fungi observed in this study (Fig. 4 & Data S4), were positively
640 correlated with the soil organic C mineralization rate, while those of *Agaricales* and
641 *Helotiales*, the negative eP responders of fungi, were negatively correlated (Wang *et al.*
642 *et al.*, 2021, Zhang *et al.*, 2021). Our results coincided with the finding that potential

643 activities of fungi-mediated C degradation enzymes, such as those degrading chitin,
644 phosphodiester, lignin, cellulose, and xylan, were positively correlated with soil
645 moisture (A'Bear *et al.*, 2014). Intriguingly, the role of fungal community composition
646 in regulating soil C was linked to the C degradation genes enriched under eP and
647 bacteriophage genes (Fig. 6A), implying possible complex interplay among
648 bacteriophages, bacteria, and fungi in mediating the response of soil C turnover to
649 long-term eP.

650 Alternatively, nutrient leaching, occurring through soil erosion or soil C migration
651 from terrestrial to riverine ecosystems, can also contribute to soil C loss (Frank *et al.*,
652 2015), though we do not suspect this to be the main cause of decreased soil C in this
653 experiment. Although we did not measure the magnitude of C leaching directly, we
654 could estimate it by analyzing soil N data because soil C and N leaching often happen
655 simultaneously (He *et al.*, 2017). The eP treatment itself did not alter N inputs either,
656 since the supplemental water was from the domestic water supply and was added
657 through drip irrigation and overhead sprinklers without flushing atmospheric N. Soil
658 total N was not decreased by eP unless N deposition was elevated and the
659 temperature was ambient (Fig. 1B), suggesting that N leaching might be only evident
660 when more N was added to soil. Therefore, change in leaching, if any, might have
661 played a minor role in soil C loss under eP as compared to aP.

662

663 **Implications and future directions**

664 Our findings have important implications for predicting the ecological consequences

665 of climate change. Long-term eP altered both microbial compositions and functional
666 traits, which differed from short-term effects (Docherty *et al.*, 2011, Gutknecht *et al.*,
667 2012). Therefore, the effects of long-term climate change on ecosystems are crucial
668 for future studies (Melillo *et al.*, 2017). In addition, we revealed a potential role of
669 the viral shunt in regulating soil C cycling, underscoring the importance of including
670 soil viruses in microbial analysis. Although numerous studies have reported that eP
671 increases soil C storage, our results demonstrate that long-term eP combined with
672 eCO₂ induced soil C loss in this type of water-limited annual grassland via
673 microbe-plant-soil interplay. Therefore, a long-term increase in precipitation and CO₂
674 induced by climate change in some regions could generate a previously unexpected
675 loss of soil C. This could represent an important positive feedback to climate change
676 that has been overlooked so far. However, further research is necessary to determine
677 whether soil C loss and associated regulating mechanisms will persist for longer time
678 scales or in other ecosystems.

679 **Acknowledgments**

680 The authors wish to thank the staff of the Jasper Ridge Global Change Experiment for
681 site preservation and sampling assistance. This study was supported National Natural
682 Science Foundation of China grant (41825016/32161123002/42007297), Office of
683 the Vice President for Research at the University of Oklahoma, Office of Science and
684 Office of Biological and Environmental Research (DOE-BER) of the U.S. Department of
685 Energy Genomic Science Program grant DE-SC0004601 and DE-SC0010715, the US
686 National Science Foundation grant DEB-0092642/0445324, the Packard Foundation,
687 the Morgan Family Foundation, the Second Tibetan Plateau Scientific Expedition and
688 Research (STEP) Program grant 2019QZKK0503, Guangdong Basis and Applied Basic
689 Research Foundation grant (2019A1515110345/2021A1515011497), Science &
690 Technology Fundamental Resources Investigation Program grant 2019FY100700, the
691 Key Technology R&D Program of Jiangxi Province grant 20223BBG74S02, G. Evelyn
692 Hutchinson postdoctoral fellowship from Yale Institute for Biospheric Studies at Yale
693 University, the Simons Foundation postdoctoral fellowship in Marine Microbial
694 Ecology, the French Institute of Agriculture, Food and Environment Research (INRAE,
695 ECODIV Department), and the French CNRS/INSU - EC2CO Program (project
696 INTERACT).

697

698 **Data availability statement**

699 The data that support the findings of this study are open available in Zenodo at
700 <https://doi.org/10.5281/zenodo.7964426>. GeoChip data are available in the NCBI

701 GEO database at <https://www.ncbi.nlm.nih.gov/geo/>, accession number GSE107168.

702 MiSeq data are available in the NCBI SRA database at

703 <https://www.ncbi.nlm.nih.gov/sra>, accession number PRJNA419455. Scripts are

704 available at

705 <https://github.com/MengmengWang223/Microbial-functional-trait-longterm-precipi>

706 tation-JRGCE.

707

708 **Competing interests**

709 The authors declare no competing interests.

710

711 **References**

- 712 A'bear AD, Jones TH, Kandeler E, Boddy L (2014) Interactive effects of temperature and soil
713 moisture on fungal-mediated wood decomposition and extracellular enzyme activity. *Soil*
714 *Biology and Biochemistry*, **70**, 151-158.
- 715 Abarenkov K, Zirk A, Piirmann T, Pöhönen R, Ivanov F, Nilsson RH, Kõljalg U (2021) *UNITE*
716 *QIIME release for Fungi*, UNITE Community.
- 717 Barnard R, Le Roux X, Hungate BA, Cleland EE, Blankinship JC, Barthes L, Leadley PW (2006)
718 Several components of global change alter nitrifying and denitrifying activities in an
719 annual grassland. *Functional Ecology*, **20**, 557-564.
- 720 Barnard R, Osborne CA, Firestone MK (2013) Responses of soil bacterial and fungal
721 communities to extreme desiccation and rewetting. *The ISME Journal*, **7**, 2229-2241.
- 722 Bolyen E, Rideout JR, Dillon MR *et al.* (2019) Reproducible, interactive, scalable and
723 extensible microbiome data science using QIIME 2. *Nature Biotechnology*, **37**, 852-857.
- 724 Brown JR, Blankinship JC, Niboyet A *et al.* (2012) Effects of multiple global change treatments
725 on soil N₂O fluxes. *Biogeochemistry*, **109**, 85-100.
- 726 Chou WW, Silver WL, Jackson RD, Thompson AW, Allen-Diaz B (2008) The sensitivity of
727 annual grassland carbon cycling to the quantity and timing of rainfall. *Global Change*
728 *Biology*, **14**, 1382-1394.
- 729 Corringham TW, Ralph FM, Gershunov A, Cayan DR, Talbot CA (2019) Atmospheric rivers
730 drive flood damages in the western United States. *Science Advances*, **5**, eaax4631.
- 731 Coutinho FH, Silveira CB, Gregoracci GB *et al.* (2017) Marine viruses discovered via
732 metagenomics shed light on viral strategies throughout the oceans. *Nature*
733 *Communications*, **8**, 15955.
- 734 Dahlin KM, Asner GP, Field CB (2013) Environmental and community controls on plant
735 canopy chemistry in a Mediterranean-type ecosystem. *Proceedings of the National*
736 *Academy of Sciences of the United States of America*, **110**, 6895-6900.
- 737 Dang C, Kong F, Li Y, Jiang Z, Xi M (2022) Soil inorganic carbon dynamic change mediated by
738 anthropogenic activities: An integrated study using meta-analysis and random forest
739 model. *Science of the Total Environment*, **835**, 155463.
- 740 De'ath G (2007) Boosted trees for ecological modeling and prediction. *Ecology*, **88**, 243-251.
- 741 Derner JD, Schuman GE (2007) Carbon sequestration and rangelands: A synthesis of land
742 management and precipitation effects. *Journal of Soil and Water Conservation*, **62**, 77-85.
- 743 Docherty KM, Balser TC, Bohannan BJM, Gutknecht JLM (2011) Soil microbial responses to
744 fire and interacting global change factors in a California annual grassland.
745 *Biogeochemistry*, **109**, 63-83.
- 746 Dukes JS, Chiariello NR, Cleland EE *et al.* (2005) Responses of grassland production to single
747 and multiple global environmental changes. *PLoS Biology*, **3**, e319.
- 748 Edgar RC (2018) Updating the 97% identity threshold for 16S ribosomal RNA OTUs.
749 *Bioinformatics*, **34**, 2371-2375.
- 750 Ernst L, Steinfeld B, Barayeu U *et al.* (2022) Methane formation driven by reactive oxygen
751 species across all living organisms. *Nature*, **603**, 482-487.
- 752 Falloon P, Jones CD, Ades M, Paul K (2011) Direct soil moisture controls of future global soil
753 carbon changes: An important source of uncertainty. *Global Biogeochemical Cycles*, **25**,

754 GB3010.

755 Feng J, Turner BL, Wei K *et al.* (2018) Divergent composition and turnover of soil organic
756 nitrogen along a climate gradient in arid and semiarid grasslands. *Geoderma*, **327**, 36-44.

757 Flanagan LB, Wever LA, Carlson PJ (2002) Seasonal and interannual variation in carbon
758 dioxide exchange and carbon balance in a northern temperate grassland. *Global Change*
759 *Biology*, **8**, 599-615.

760 Fouquier J, Rideout JR, Bolyen E *et al.* (2016) Ghost-tree: creating hybrid-gene phylogenetic
761 trees for diversity analyses. *Microbiome*, **4**, 11.

762 Frank D, Reichstein M, Bahn M *et al.* (2015) Effects of climate extremes on the terrestrial
763 carbon cycle: concepts, processes and potential future impacts. *Global Change Biology*,
764 **21**, 2861-2880.

765 Gao Y, Ding J, Yuan M *et al.* (2021) Long-term warming in a Mediterranean-type grassland
766 affects soil bacterial functional potential but not bacterial taxonomic composition. *npj*
767 *Biofilms and Microbiomes*, **7**, 17.

768 Goberna M, Navarro-Cano JA, Valiente-Banuet A, Garcia C, Verdu M (2014) Abiotic stress
769 tolerance and competition-related traits underlie phylogenetic clustering in soil bacterial
770 communities. *Ecology Letters*, **17**, 1191-1201.

771 Gulev SK, Thorne PW, J. Ahn FJD *et al.* (2021) *Changing State of the Climate System. In*
772 *Climate Change 2021: The Physical Science Basis. Contribution of Working Group I to the*
773 *Sixth Assessment Report of the Intergovernmental Panel on Climate Change*
774 *[Masson-Delmotte, V., P. Zhai, A. Pirani, S.L. Connors, C. Péan, S. Berger, N. Caud, Y. Chen,*
775 *L. Goldfarb, M.I. Gomis, M. Huang, K. Leitzell, E. Lonnoy, J.B.R. Matthews, T.K. Maycock, T.*
776 *Waterfield, O. Yelekçi, R. Yu, and B. Zhou (eds.)], Cambridge, United Kingdom and New*
777 *York, NY, USA, Cambridge University Press.*

778 Guo X, Feng J, Shi Z *et al.* (2018) Climate warming leads to divergent succession of grassland
779 microbial communities. *Nature Climate Change*, **8**, 813-818.

780 Guo X, Zhou X, Hale L *et al.* (2019) Climate warming accelerates temporal scaling of grassland
781 soil microbial biodiversity. *Nature Ecology & Evolution*, **3**, 612-619.

782 Gutknecht JLM, Field CB, Balser TC (2012) Microbial communities and their responses to
783 simulated global change fluctuate greatly over multiple years. *Global Change Biology*, **18**,
784 2256-2269.

785 He Y, Lehndorff E, Amelung W, Wassmann R, Alberto MC, Von Unold G, Siemens J (2017)
786 Drainage and leaching losses of nitrogen and dissolved organic carbon after introducing
787 maize into a continuous paddy-rice crop rotation. *Agriculture, Ecosystems & Environment*,
788 **249**, 91-100.

789 Henry HA, Juarez JD, Field CB, Vitousek PM (2005) Interactive effects of elevated CO₂, N
790 deposition and climate change on extracellular enzyme activity and soil density
791 fractionation in a California annual grassland. *Global Change Biology*, **11**, 1808-1815.

792 Horz H-P, Barbrook A, Field CB, Bohannan BJ (2004) Ammonia-oxidizing bacteria respond to
793 multifactorial global change. *Proceedings of the National Academy of Sciences of the*
794 *United States of America*, **101**, 15136-15141.

795 Hubbell SP (2001) *The unified neutral theory of biodiversity and biogeography (MPB-32)*,
796 Princeton, Princeton Univ. Press.

797 Huntington TG (2006) Evidence for intensification of the global water cycle: Review and

798 synthesis. *Journal of Hydrology*, **319**, 83-95.

799 Iwasa Y, Roughgarden J (1984) Shoot/root balance of plants: Optimal growth of a system with
800 many vegetative organs. *Theoretical Population Biology*, **25**, 78-105.

801 Le Roux X, Bouskill NJ, Niboyet A *et al.* (2016) Predicting the responses of soil nitrite-oxidizers
802 to multi-factorial global change: a trait-based approach. *Frontiers in Microbiology*, **7**, 628.

803 Liu Y, Wang C, He N *et al.* (2017) A global synthesis of the rate and temperature sensitivity of
804 soil nitrogen mineralization: latitudinal patterns and mechanisms. *Global Change Biology*,
805 **23**, 455-464.

806 Louca S, Doebeli M (2018) Efficient comparative phylogenetics on large trees. *Bioinformatics*,
807 **34**, 1053-1055.

808 Love MI, Huber W, Anders S (2014) Moderated estimation of fold change and dispersion for
809 RNA-seq data with DESeq2. *Genome Biology*, **15**, 550.

810 Ma B, Zhou X, Zhang Q *et al.* (2019) How do soil micro-organisms respond to N, P and NP
811 additions? Application of the ecological framework of (co-)limitation by multiple
812 resources. *Journal of Ecology*, **107**, 2329-2345.

813 Magoč T, Salzberg SL (2011) FLASH: fast length adjustment of short reads to improve genome
814 assemblies. *Bioinformatics*, **27**, 2957-2963.

815 Malik AA, Martiny JBH, Brodie EL, Martiny AC, Treseder KK, Allison SD (2020) Defining
816 trait-based microbial strategies with consequences for soil carbon cycling under climate
817 change. *The ISME Journal*, **14**, 1-9.

818 Malik AA, Puissant J, Buckeridge KM *et al.* (2018) Land use driven change in soil pH affects
819 microbial carbon cycling processes. *Nature Communications*, **9**, 1-10.

820 Marti JA, Gorley RN, Clarke RK (2008) *PERMANOVA+ for PRIMER: Guide to Software and*
821 *Statistical Methods*, Plymouth, UK, Primer-e.

822 Martiny AC, Treseder K, Pusch G (2013) Phylogenetic conservatism of functional traits in
823 microorganisms. *The ISME Journal*, **7**, 830-838.

824 Mason RE, Craine JM, Lany NK *et al.* (2022) Evidence, causes, and consequences of declining
825 nitrogen availability in terrestrial ecosystems. *Science*, **376**, eabh3767.

826 Melillo JM, Frey SD, Deangelis KM *et al.* (2017) Long-term pattern and magnitude of soil
827 carbon feedback to the climate system in a warming world. *Science*, **358**, 101-105.

828 Morrow JG, Huggins DR, Reganold JP (2017) Climate change predicted to negatively influence
829 surface soil organic matter of dryland cropping systems in the inland Pacific Northwest,
830 USA. *Frontiers in Ecology and Evolution*, **5**, 10.

831 Nelson JA, Morgan JA, Lecain DR, Mosier AR, Milchunas DG, Parton BA (2004) Elevated CO₂
832 increases soil moisture and enhances plant water relations in a long-term field study in
833 semi-arid shortgrass steppe of Colorado. *Plant and Soil*, **259**, 169-179.

834 Niboyet A, Brown JR, Dijkstra P *et al.* (2011a) Global change could amplify fire effects on soil
835 greenhouse gas emissions. *PloS One*, **6**, e20105.

836 Niboyet A, Le Roux X, Dijkstra P *et al.* (2011b) Testing interactive effects of global
837 environmental changes on soil nitrogen cycling. *Ecosphere*, **2**, art56.

838 Nielsen UN, Ball BA (2015) Impacts of altered precipitation regimes on soil communities and
839 biogeochemistry in arid and semi-arid ecosystems. *Global Change Biology*, **21**, 1407-1421.

840 Ning D, Deng Y, Tiedje JM, Zhou J (2019) A general framework for quantitatively assessing
841 ecological stochasticity. *Proceedings of the National Academy of Sciences of the United*

842 States of America, **116**, 16892-16898.

843 Ochoa-Hueso R, Arca V, Delgado-Baquerizo M *et al.* (2020) Links between soil microbial
844 communities, functioning, and plant nutrition under altered rainfall in Australian
845 grassland. *Ecological Monographs*, **90**, e01424.

846 Placella SA, Brodie EL, Firestone MK (2012) Rainfall-induced carbon dioxide pulses result
847 from sequential resuscitation of phylogenetically clustered microbial groups. *Proceedings*
848 *of the National Academy of Sciences of the United States of America*, **109**, 10931-10936.

849 Price MN, Dehal PS, Arkin AP (2010) FastTree 2--approximately maximum-likelihood trees for
850 large alignments. *PloS One*, **5**, e9490.

851 Prosser JI, Bohannan BJ, Curtis TP *et al.* (2007) The role of ecological theory in microbial
852 ecology. *Nature Reviews Microbiology*, **5**, 384-392.

853 Qi Q, Haowei Y, Zhang Z *et al.* (2021) Microbial functional responses explain alpine soil
854 carbon fluxes under future climate scenarios. *mBio*, **12**, e00761-00720.

855 Quast C, Pruesse E, Yilmaz P *et al.* (2013) The SILVA ribosomal RNA gene database project:
856 improved data processing and web-based tools. *Nucleic Acids Research*, **41**, D590-D596.

857 Reichstein M, Bahn M, Ciais P *et al.* (2013) Climate extremes and the carbon cycle. *Nature*,
858 **500**, 287-295.

859 Rosseel Y (2012) lavaan: an R package for structural equation modeling. *Journal of Statistical*
860 *Software*, **48**, 1 - 36.

861 Schuur EaG, Matson PA (2001) Net primary productivity and nutrient cycling across a mesic
862 to wet precipitation gradient in Hawaiian montane forest. *Oecologia*, **128**, 431-442.

863 Shaw AN, Cleveland CC (2020) The effects of temperature on soil phosphorus availability and
864 phosphatase enzyme activities: a cross-ecosystem study from the tropics to the Arctic.
865 *Biogeochemistry*, **151**, 113-125.

866 Shaw MR, Zavaleta ES, Chiariello NR, Cleland EE, Mooney HA, Field CB (2002) Grassland
867 responses to global environmental changes suppressed by elevated CO₂. *Science*, **298**,
868 1987-1990.

869 Shi Y, Wang J, Ao Y *et al.* (2021) Responses of soil N₂O emissions and their abiotic and biotic
870 drivers to altered rainfall regimes and co-occurring wet N deposition in a semi-arid
871 grassland. *Global Change Biology*, **27**, 4894-4908.

872 Sokol NW, Slessarev E, Marschmann GL *et al.* (2022) Life and death in the soil microbiome:
873 how ecological processes influence biogeochemistry. *Nature Reviews Microbiology*, **20**,
874 415-430.

875 Stevenson S, Coats S, Touma D, Cole J, Lehner F, Fasullo J, Otto-Bliesner B (2022) Twenty-first
876 century hydroclimate: A continually changing baseline, with more frequent extremes.
877 *Proceedings of the National Academy of Sciences of the United States of America*, **119**,
878 e2108124119.

879 Strong AL, Johnson TP, Chiariello NR, Field CB (2017) Experimental fire increases soil carbon
880 dioxide efflux in a grassland long-term multifactor global change experiment. *Global*
881 *Change Biology*, **23**, 1975-1987.

882 Sullivan MJ, Thomsen MA, Suttle KB (2016) Grassland responses to increased rainfall depend
883 on the timescale of forcing. *Global Change Biology*, **22**, 1655-1665.

884 Tiedje JM, Bruns MA, Casadevall A *et al.* (2022) Microbes and Climate Change: a Research
885 Prospectus for the Future. *mBio*, **13**, e00800-00822.

886 Wang M, Ding J, Sun B *et al.* (2018) Microbial responses to inorganic nutrient amendment
887 overridden by warming: Consequences on soil carbon stability. *Environ Microbiol*, **20**,
888 2509-2522.

889 Wang R, Dorodnikov M, Yang S *et al.* (2015) Responses of enzymatic activities within soil
890 aggregates to 9-year nitrogen and water addition in a semi-arid grassland. *Soil Biology*
891 *and Biochemistry*, **81**, 159-167.

892 Wang X, Bian Q, Jiang Y, Zhu L, Chen Y, Liang Y, Sun B (2021) Organic amendments drive shifts
893 in microbial community structure and keystone taxa which increase C mineralization
894 across aggregate size classes. *Soil Biology and Biochemistry*, **153**, 108062.

895 Williamson KE, Fuhrmann JJ, Wommack KE, Radosevich M (2017) Viruses in Soil Ecosystems:
896 An Unknown Quantity Within an Unexplored Territory. *Annual Review of Virology*, **4**,
897 201-219.

898 Xu L, Naylor D, Dong Z *et al.* (2018) Drought delays development of the sorghum root
899 microbiome and enriches for monoderm bacteria. *Proceedings of the National Academy*
900 *of Sciences of the United States of America*, **115**, E4284-E4293.

901 Yang S, Zheng Q, Yang Y *et al.* (2020) Fire affects the taxonomic and functional composition
902 of soil microbial communities, with cascading effects on grassland ecosystem functioning.
903 *Global Change Biology*, **26**, 431-442.

904 Yang Y, Gao Y, Wang S *et al.* (2014) The microbial gene diversity along an elevation gradient of
905 the Tibetan grassland. *The ISME Journal*, **8**, 430-440.

906 Zavaleta ES, Shaw MR, Chiariello NR, Mooney HA, Field CB (2003) Additive effects of
907 simulated climate changes, elevated CO₂, and nitrogen deposition on grassland diversity.
908 *Proceedings of the National Academy of Sciences of the United States of America*, **100**,
909 7650-7654.

910 Zhang J, Gao Q, Zhang Q *et al.* (2017) Bacteriophage-prokaryote dynamics and interaction
911 within anaerobic digestion processes across time and space. *Microbiome*, **5**, 57.

912 Zhang S, Fang Y, Luo Y *et al.* (2021) Linking soil carbon availability, microbial community
913 composition and enzyme activities to organic carbon mineralization of a bamboo forest
914 soil amended with pyrogenic and fresh organic matter. *Science of the Total Environment*,
915 **801**, 149717.

916 Zhou J, Bruns MA, Tiedje JM (1996) DNA recovery from soils of diverse composition. *Applied*
917 *and Environmental Microbiology*, **62**, 316-322.

918 Zhou J, Xue K, Xie J *et al.* (2012) Microbial mediation of carbon-cycle feedbacks to climate
919 warming. *Nature Climate Change*, **2**, 106-110.

920 Zhu K, Chiariello NR, Tobeck T, Fukami T, Field CB (2016) Nonlinear, interacting responses to
921 climate limit grassland production under global change. *Proceedings of the National*
922 *Academy of Sciences of the United States of America*, **113**, 10589-10594.

923

Table 1. The consenTRAIT analysis showing phylogenetic conservation of microbial responses to eP.

Kingdom	Response	τ_D^*	<i>P</i> -value†
Bacteria	Increase	0.116	< 0.001
	Decrease	0.063	< 0.001
Fungi	Increase	0.190	0.211
	Decrease	0.267	0.004

* τ_D is the mean phylogenetic depth at which the response is conserved across clades.

†Significance values were estimated using 999 randomizations (*P* values < 0.050 in bold). A significant value indicates a greater mean depth than randomization, indicating deeper-rooting conservation across clades.

Figure legends

Figure 1. The effects of the eP treatment on soil total C, soil total N, CO₂ efflux, and plant variables in the 2nd–14th year after the experiment treatment began. (a), Soil total C in phase I over the 2nd–9th years and in phase II over the 10th–14th years. (b), Soil total N. (c), Soil C: N ratio, calculated as the mass ratio of soil total C to N. (d), ANPP, BNPP, and NPP. As BNPP in the 9th year was not measured, only data in Years 2nd–8th and 10th–14th are displayed. (e), Soil total C under different warming treatments. (f), Soil total C in phase II over 10th–14th years under different CO₂ and warming treatments. (g), Soil CO₂ efflux in the 14th year. (h), BNPP under different CO₂ and warming treatments. (i), NPP under different CO₂ and warming treatments. Means and standard errors are indicated. Treatments: all, across other climate change factors; aC, ambient CO₂; eC, elevated CO₂; aW, ambient temperature, eW, warming; aN, ambient N; eN, N deposition. *** denotes $P < 0.001$, ** denotes $P < 0.010$, * denotes $P < 0.050$, and # denotes $P < 0.100$.

Figure 2. The effects of the long-term eP treatment on C degradation genes, viral genes, and stress response genes. (a), Percent changes of individual C degradation genes. Labels represent targeted substrates. The percent change represents the effect size of relative abundances calculated as follows: % effect = $100\% \times (eP - aP)/aP$. (b), Percent changes of functional subcategories for prokaryotic and eukaryotic viral genes. (c), Percent changes of individual stress response genes. Only significantly and

marginally significantly changed genes (FDR corrected $P < 0.100$) are shown. The error bar represents the standard error ($n = 32$). *** denotes $P < 0.001$, ** denotes $P < 0.010$, * denotes $P < 0.050$, and # denotes $P < 0.100$.

Figure 3. The phylogenetic tree of bacterial ASVs significantly changed by eP. The inner colored ring represents the phylum of each ASV. The middle ring of colored bars represents the relative \log_2 -fold change of each ASV in eP quadrants compared with aP quadrants. The outer ring displays the mean relative abundance of each ASV. The colored branches represent the phylogenetically clustered groups (families and higher taxonomic level clades), with orange branches indicating increased groups and blue-green branches indicating decreased groups.

Figure 4. The phylogenetic tree of fungal ASVs significantly changed by eP. The inner colored ring represents the phylum of each ASV. The middle ring of colored bars represents the relative \log_2 -fold change of each ASV in eP quadrants compared with aP quadrants. The outer ring indicates the mean relative abundance of each ASV. The colored branches represent the phylogenetically clustered groups (families and higher taxonomic level clades), with orange branches indicating increased groups and blue-green branches indicating decreased groups.

Figure 5. Stochastic and deterministic factors influencing microbial communities. (a), The estimated stochastic ratio in prokaryotic community assembly. The significance of the effect for each treatment was tested by split-plot PERMANOVA. P: precipitation, C: CO₂. The significance of the eP treatment under different CO₂ regimes was tested by *t*-test. (b), The estimated stochastic ratio in fungal community assembly. (c), Environmental variables driving composition changes of ASVs and stress genes significantly altered by the eP treatment. The color gradient represents Pearson's correlation coefficients of pairwise correlations of environmental variables. The edge width corresponds to the Mantel correlation coefficients, and the edge color denotes the statistical significance of the Mantel tests. SRoot, shallow root biomass (0–15 cm); FRoot, fine root biomass (0–15 cm); DRoot, deep root biomass (15–30 cm); TRoot, total root biomass; AG, annual grass biomass; AF, annual forb biomass; PG, perennial grass biomass; PF, perennial forb biomass; AGB, aboveground biomass; TC, soil total C; TN, soil total N; Soil T, soil temperature.

Figure 6. Biotic and abiotic drivers in regulating soil total C content. (a), The structural equation model (SEM) showing the influences of the eP treatment (grey rectangle), environmental variables, and microbial profiles on soil total C. Red arrows represent significant and marginally significant positive pathways, and blue arrows represent significant and marginally significant negative pathways. The width of each arrow is proportional to the strength of the relationship and numbers near the

pathway represent the standardized path coefficients. Bootstrap-based P -values for path coefficients are indicated by *** when $P < 0.001$, ** when $P < 0.010$, * when $P < 0.050$, and # when $P < 0.100$. R^2 represents the proportion of variance explained for soil total C. (b), Standardized total effects (direct and indirect effects) based on SEM. (c), The relative influences of biotic and abiotic variables in affecting soil total C, as revealed by aggregated boosted tree (ABT) analysis. Enriched C degra. gene represents the relative abundances of increased C degradation genes shown in Fig. 2A, including those in the degradation of chitin and protein. Fungal comm. comp. refers to fungal community composition, as represented by the PC1 from the principal coordinate analysis based on the Bray-Curtis distance of the fungal ASV matrix.